Journal of Nuclear Materials 384 (2009) 38–47

Contents lists available at ScienceDirect

Journal of Nuclear Materials

journal homepage: www.elsevier.com/locate/jnucmat

Proton irradiation effect on microstructure, strain localization and iodine-induced stress corrosion cracking in Zircaloy-4

L. Fournier [a], A. Serres [a], Q. Auzoux [a,*], D. Leboulch [a], G.S. Was [b]

[a] Commissariat à l'Energie Atomique, CEA Saclay, DMN/SEMI/LCMI, 91191 Gif-Sur-Yvette, France
[b] Department of Nuclear Engineering and Radiological Sciences, University of Michigan, Ann Arbor, MI 48109, USA

ARTICLE INFO

Article history:
Received 16 July 2008
Accepted 2 October 2008

ABSTRACT

The radiation-induced microstructure, strain localization, and iodine-induced stress corrosion cracking (I-SCC) behaviour of recrystallized Zircaloy-4 proton-irradiated to 2 dpa at 305 °C was examined. <a> type dislocation loops having $1/3\langle 11\bar{2}0\rangle$ Burgers vector and a mean diameter and density of, respectively, 10 nm and 17×10^{21} m^{-3} were observed while no $Zr(Fe,Cr)_2$ precipitates amorphization or Fe redistribution were detected after irradiation. After transverse tensile testing to 0.5% macroscopic plastic strain at room temperature, almost exclusively basal channels were imaged. Statistical Schmid factor analysis shows that irradiation leads to a change in slip system activation from prismatic to basal due to a higher increase of critical resolved shear stresses for prismatic slip systems than for basal slip system. Finite element calculations suggest that dislocation channeling occurs in the irradiated proton layer at an equivalent stress close to 70% of the yield stress of the irradiated material, i.e. while the irradiated layer is still in the elastic regime for a 0.5% applied macroscopic plastic strain. Comparative constant elongation rate tensile tests performed at a strain rate of 10^{-5} s^{-1} in iodized methanol solutions at room temperature on specimens both unirradiated and proton-irradiated to 2 dpa demonstrated a detrimental effect of irradiation on I-SCC.

1. Introduction

The first fractures by pellet-cladding interactions (PCI) were observed during the 1960s in boiling water reactors (BWRs) and CANDU-type reactors [1]. With the development of barrier cladding using an inner layer of pure zirconium in BWR design in the 80s, PCI has since received little attention, excepted for power transient conditions in pressurized water reactors (PWRs). Indeed, cladding failure by iodine-induced stress corrosion cracking (I-SCC) may occur under PCI conditions during power transients in PWRs. I-SCC then results from the synergistic effect of (i) the hoop tensile stress and strain imposed on the cladding by fuel thermal expansions during power transients and (ii) corrosion by iodine released from the UO_2 fuel as a fission product [1]. In spite of numerous laboratory studies, the mechanisms controlling I-SCC are not well understood. Irradiation is believed to play a significant role in the phenomenon [2,3] but the precise mechanism by which it may affect I-SCC is not clear.

Irradiated and deformed zirconium alloys are clearly prone to dislocation channel formation [4–11] and several authors [12,13] suggested that dislocation channeling may be responsible for an increase in the I-SCC cracking susceptibility of irradiated zirconium alloys. However there is no clear consensus on the activated slip systems in irradiated zirconium alloys and there is no evidence that dislocation channeling affects I-SCC.

This work was therefore aimed at (i) contributing to the clarification on the activated slip systems in irradiated zirconium alloys and (ii) giving insights into the possible effect of channeling on I-SCC by means of proton irradiation and constant elongation rate tensile (CERT) testing in iodized methanol solution at room temperature. Several authors [4,14] already demonstrated that I-SCC in gaseous iodine environment at temperature around 300 °C is relatively well simulated by I-SCC tests performed in iodized methanol solution at room temperature. Zu et al. [15,16] also recently made the first effort to investigate the effect of proton irradiation on Zircaloy-4 in terms of microstructure, microchemistry and hardness. These authors identified an irradiation temperature range between 300 and 350 °C under which neutron irradiation effects can be reproduced by proton irradiation. In the present work, radiation-induced microstructure as well as dislocation channeling in Zircaloy-4 proton-irradiated to 2 dpa at 305 °C was investigated together with the I-SCC behaviour.

Finite element (FE) calculations were also carried out in order to guide the interpretation of the CERT tests performed on proton-irradiated Zircaloy-4 specimens.

* Corresponding author. Tel.: +33 1 69 08 18 34; fax: +33 1 69 08 93 24.
E-mail address: quentin.auzoux@cea.fr (Q. Auzoux).

0022-3115/$ - see front matter © 2008 Elsevier B.V. All rights reserved.
doi:10.1016/j.jnucmat.2008.10.001

2. Experimental procedure

Fully recrystallized Zircaloy-4 in the form of a 6 mm thick sheet was provided by CEZUS. The chemical composition of this material is given in Table 1 and the grain size was measured to be around 7 μm. The {0002} and {10$\bar{1}$0} pole figures, determined by standard X-ray diffraction technique and given in Fig. 1, illustrate the strong and classical texture of the rolled and recrystallized Zircaloy-4 sheet with *c* axis 35° to the normal direction (ND) in the transverse-normal (TD-ND) plane.

Two types of samples were proton-irradiated: transmission electron microscopy (TEM) bars and tensile specimens. A drawing of the sample design is provided in Fig. 2. All samples were fabricated by electric discharge machining in the transverse direction in the TD-LD plane. Prior to irradiation, specimens were mechanically wet-polished using SiC paper (grit 320-2400). Proton irradiations were conducted at the Michigan ion beam laboratory at the University of Michigan. Samples were mounted on a specially designed irradiation stage attached to the main target chamber of a General Ionex Tandetron accelerator. Temperature control was achieved by mounting the samples on a copper block with an indium liquid metal coupling to facilitate heat conduction between the samples and the stage. The sample temperature during irradiation was maintained at 305 ± 10 °C. Irradiations were conducted to a nominal dose of 2 dpa with 2 MeV protons at a dose rate of approximately 2.6×10^{-5} dpa/s, resulting in a nearly uniform damage rate throughout the first 25 μm of the proton range (~30 μm). Both tensile and TEM specimens were irradiated, in their center part, on an 11 mm length. The temperature for proton irradiations was chosen to partially compensate for the damage-rate difference and to produce irradiation damage in materials relevant to LWR cores. Experimental doses and dose rates were calculated using TRIM97 with a threshold displacement energy of 40 eV.

Table 1
Chemical composition of the Zircaloy-4 alloy used in this study (in weight percent).

Sn	Fe	Cr	O	Zr
1.35	0.23	0.1	0.12	Bal.

Hardening in proton-irradiated samples was measured by Vickers indentation (MICROMET II) with a load of 25 g. This low load was used to confine the plastic zone ahead of the indenter tip to a depth within the proton range to ensure that unirradiated material is not being sampled.

Three-mm TEM discs were cut using a slurry drill cutter. TEM discs were then prepared by electropolishing in a 10% perchloric acid and 90% methanol solution at −10 °C and 20 V. Radiation-induced microstructure was characterized using a 300 kV TECNAI30 transmission electron microscope. The dominant microstructural feature observed for all specimens was <a>-type dislocation loops having 1/3⟨11$\bar{2}$0⟩ Burgers vector. About 800 dislocation loops were imaged to obtain average loop diameter and number density. Thin foil thicknesses were determined using thickness fringes along a grain boundary.

Particular attention was paid to strain localization within dislocation channels after CERT testing at a strain rate of 10^{-5} s^{-1} up to 0.5% macroscopic plastic deformation at room temperature. Channel traces on the stereographic projection were systematically analyzed in order to identify the channeling slip system. For that purpose, the tilt conditions for the maximum contrast between the channels and the matrix were systematically recorded since they correspond to the situation where the channeling plane contains the electron beam. This method allows the unambiguous determination of the channeling slip system.

Eventual partial precipitate amorphization associated with Fe release after proton irradiation to 2 dpa at 305 °C was examined. Both conventional bright field TEM observation to detect the presence or not of an amorphous rim, and scanning TEM (STEM)/energy-dispersive X-ray spectroscopy (EDS) composition profiles on $Zr(Cr,Fe)_2$ precipitates were performed.

CERT tests were performed at a strain rate of 10^{-5} s^{-1} in iodized methanol solutions in the range 10^{-6} gram of iodine per gram of methanol (g/g) to 6×10^{-6} g/g at room temperature on both unirradiated and proton-irradiated tensile test specimens. Engineering stress-strain curves were post-processed by linearly fitting the elastic part to a Young's modulus of 92 GPa. Analysis of both the fracture and the side surfaces of specimens after CERT testing was carried out by scanning electron microscopy (SEM). Prior to SEM examination specimens were ultrasonically cleaned first in acetone and then in ethanol. Additional CERT tests were performed

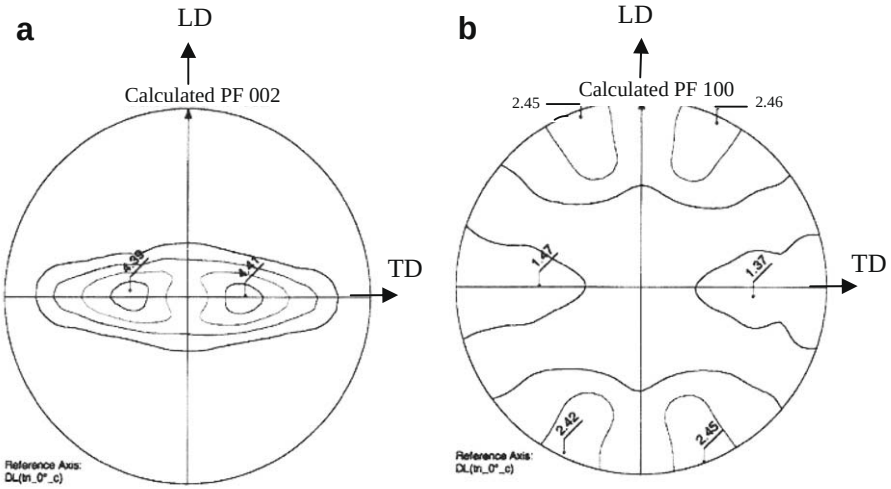

Kearns factors : $f_N = 0.601$, $f_T = 0.298$, $f_L = 0.101$

Fig. 1. (a) {0002} and (b) {10$\bar{1}$0} pole figures for the recrystallized Zircaloy-4 sheet used in this study.

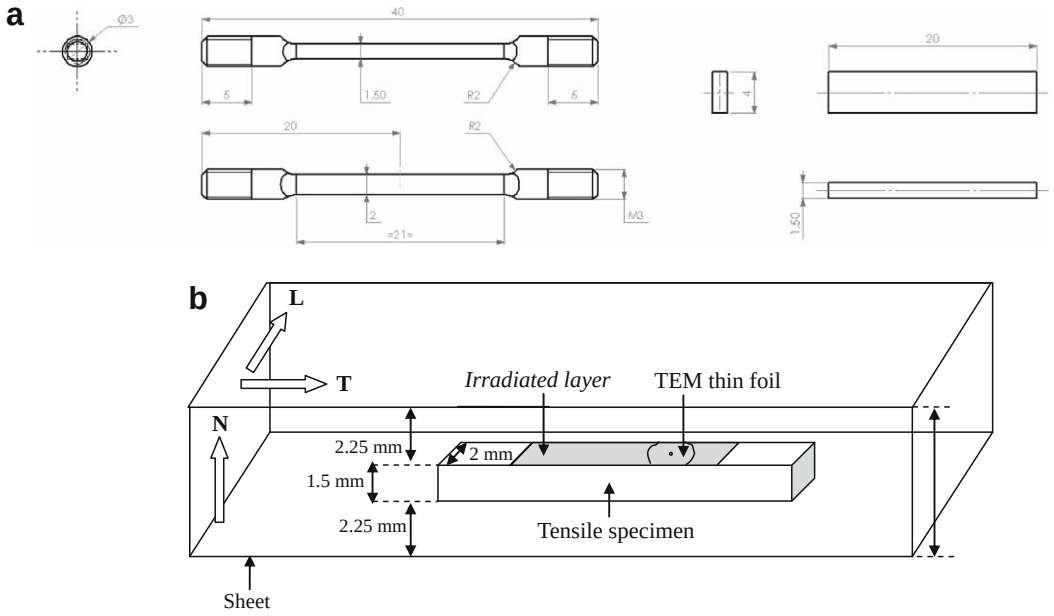

Fig. 2. Schematic of (a) the tensile test specimens and the TEM bars used in this study (b) the orientation of the sample in respect to the longitudinal (L), transverse (T) and normal (N) directions of the sheet.

at 10^{-5} s^{-1} in air in order to determine the mechanical behaviour of the studied material.

3. Numerical procedure

Finite element (FE) calculations were performed in order to estimate stress and strain distributions in tensile specimens during CERT tests, paying particular attention to the thin 30 μm proton-irradiated layer. Constitutive equations, geometry and mesh are described in this section.

Both irradiated and unirradiated parts of the specimens were considered as homogeneous materials, i.e. grains were not modelled individually. Anisotropic elastic-plastic constitutive equations for irradiated and unirradiated Zircaloy-4 were, respectively, derived from literature data and from CERT tests carried-out in this study. Because of the lattice structure and the crystallographic texture of Zircaloy-4 plates, mechanical behaviour was assumed to be orthotropic. Principal directions were defined as longitudinal (L), transverse (T) and normal (N) directions, which are similar to axial (z), tangential (θ) and radial (r) directions of a fuel cladding tube.

Plastic equivalent stress σ^* threshold was described by Hill's model:

$$\sigma^* = \sqrt{H_N(\sigma_T - \sigma_L)^2 + H_T(\sigma_L - \sigma_N)^2 + H_L(\sigma_N - \sigma_T)^2} \quad (1)$$

where H_N, H_T et H_L are the Hill's parameters (with the convention $H_N + H_T = 1$) and σ_N, σ_T, and σ_L are the principal stresses.

Plastic strain increment in a given direction ($d\varepsilon_i$) as a function of the equivalent plastic strain increment ($d\varepsilon^*$) was given by the normality equation:

$$d\varepsilon_i = \frac{\partial \sigma^*}{\partial \sigma_i} d\varepsilon^*. \quad (2)$$

Using Eqs. (1) and (2) for uniaxial tensile test in the transverse direction gave the following relations:

$$\sigma^{T^*} = \sigma_T^T \sqrt{H_N + H_L}, \quad (3)$$

$$\varepsilon_T^T = \varepsilon^{T^*} \sqrt{H_N + H_L}, \quad (4)$$

$$\alpha = \frac{\varepsilon_N^T}{\varepsilon_L^T} = \frac{H_L}{H_N}. \quad (5)$$

Following Limon et al. [17] and Mahmood and Murty [18], values for H_L and H_N were, respectively, fixed at 0.20 and 0.75 for unirradiated Zircaloy-4. This choice led to $\alpha = 0.27$, which is consistent with the measurements made on fracture surface of CERT specimens tested in air. H_L and H_N parameters values were fixed at 0.5 for irradiated Zircaloy-4 since it exhibits lower anisotropy than unirradiated Zircaloy-4 [19].

A simple power like plastic strain hardening constitutive equation was selected:

$$\sigma^* = A_0 + B_0 \varepsilon^{*r_0}, \quad (6)$$

A_0, B_0, and r_0 were chosen in order to fit the true stress-strain curve obtained after CERT testing in air in the transverse direction for unirradiated Zircaloy-4. A_0, B_0, and r_0 for irradiated Zircaloy-4 were chosen based on the data obtained by Morize et al. [20] on recrystallized Zircaloy-4 neutron irradiated to 10^{25} n/m^2 and considering an almost perfectly plastic behaviour. Chosen A_0, B_0, and r_0 values for both un-irradiated and irradiated Zircaloy-4 are summarized in Table 2.

Elastic part of the mechanical behaviour was assumed to be isotropic and independent from irradiation. Young's modulus and Poisson ratio values were, respectively, set to 92 GPa and 0.3.

Only one quarter of the tensile specimen was modelled due to symmetry. Thickness and length of the irradiated layer were, respectively, set to 30 μm and 11 mm. Elements were 8 nodes rectangular with 8 Gauss points. An illustration of the mesh is displayed in Fig. 3. Particularly fine elements were used near the boundaries of the irradiated layer. Four elements were used in the 30 μm thickness of the proton-irradiated layer.

Table 2
Constitutive equations parameters used for the finite element analysis.

	A_0 (MPa)	B_0 (MPa)	r_0
Un-irradiated Zircaloy-4	340	35	0.52
Proton-irradiated Zircaloy-4	740	8	0.01

4. Results

4.1. Radiation-induced microstructure and hardening

Mean loop diameter and density of, respectively, 10 nm and 17×10^{21} m^{-3} were determined for Zircaloy-4 proton-irradiated to 2 dpa. Typical TEM bright field image of dislocation loops and loop diameter distribution are displayed in Fig. 4(a) and (b), respectively. As shown in Table 3, the mean loop diameter and density determined in this study are consistent with that determined by Zu et al. [15,16], Régnard et al. [11] and Northwood et al. [21] for, respectively, Zircaloy-4 proton-irradiated to 2 dpa at 350 °C, Zircaloy-4 neutron-irradiated to 0.6×10^{25} n/m^2 at 280 °C, and Zircaloy-2 neutron-irradiated to 1×10^{25} n/m^2 at 342 °C.

In this study of Zircaloy-4 proton-irradiated to 2 dpa at 305 °C, no $Zr(Fe,Cr)_2$ precipitate amorphization and Fe redistribution were observed. This result is also consistent with the observations of Zu et al. [15,16] that reported a very thin (5–10 nm) amorphous rim on $Zr(Fe,Cr)_2$ precipitates after Zircaloy-4 proton irradiation to 5 dpa at 310 °C.

The measured hardness of Zircaloy-4 before and after proton irradiation to 2 dpa at 305 °C are displayed in Table 3. Radiation-induced increase in hardness is in good agreement with that measured after proton irradiation of Zircaloy-4 to 2 dpa at 350 °C [15,16].

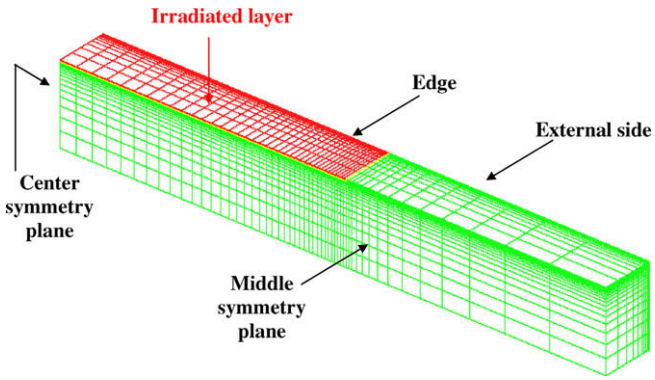

Fig. 3. Mesh corresponding to one quarter of the irradiated tensile specimen; the irradiated layer is coloured in red; un-irradiated part is coloured in green. For interpretation of the references to color in this figure legend, the reader is referred to the web version of this article.

4.2. Local stress and strain analysis

Equivalent plastic strain and equivalent stress are plotted in Figs. 5 and 6, respectively, at 0.5% and 1.1% macroscopic plastic strain. As expected, because of the higher yield stress of the irradiated material, the irradiated layer is still in the elastic regime at 0.5% macroscopic plastic strain, whereas unirradiated material is already in the plastic regime. Equivalent stress in the irradiated layer is around 525 MPa, which represents 70% of the yield stress; whereas equivalent stress in the unirradiated part is lower (around 350 MPa). The irradiated layer enters in plasticity at 1.1% macroscopic plastic strain. Calculations also indicate that the unirradiated part below the irradiated layer is not as strained as the unirradiated part in the rest of the specimen, suggesting that the thin irradiated layer significantly reinforces the center of the specimen in comparison to the ends of the specimen.

As illustrated in Fig. 7, plastic deformation of the unirradiated part induces lateral compressive stress in the irradiated layer. It is worth noticing that this compressive stress is larger in the middle than at the edge of the irradiated layer. As illustrated in Fig. 8, stress tri-axiality ratio (defined as 1/3 trace(σ)/σ^*) is significantly higher near the edge than in the middle of the irradiated layer. Stress state in the un-irradiated part remains globally uni-axial away from the irradiated part.

4.3. Radiation-induced strain localization

The results of TEM observations of dislocation microstructure in Zircaloy-4 proton-irradiated to 2 dpa after CERT testing at a strain rate of 10^{-5} s^{-1} 0.5% macroscopic plastic strain are summarized in Table 4. As shown in Fig. 9, a large number of defect-reduced channels were imaged. Ten grains out of the 40 studied grains were determined to contain basal channels by using the trace analysis method and the contrast criterion while only one grain was determined to contain one prismatic channel. These observations are in good agreement with the results of Fregonese et al. [4], Régnard et al. [11] and more recently Onimus et al. [10] who also observed basal channeling after transverse tensile testing. In contrast, Adamson and Bell [9] reported prismatic and pyramidal channels after transverse tensile testing on Zircaloy-2. The stereographic projections for no tilt (Fig. 10(b)) and (0°,−10°) tilt (Fig. 10(c)) associated

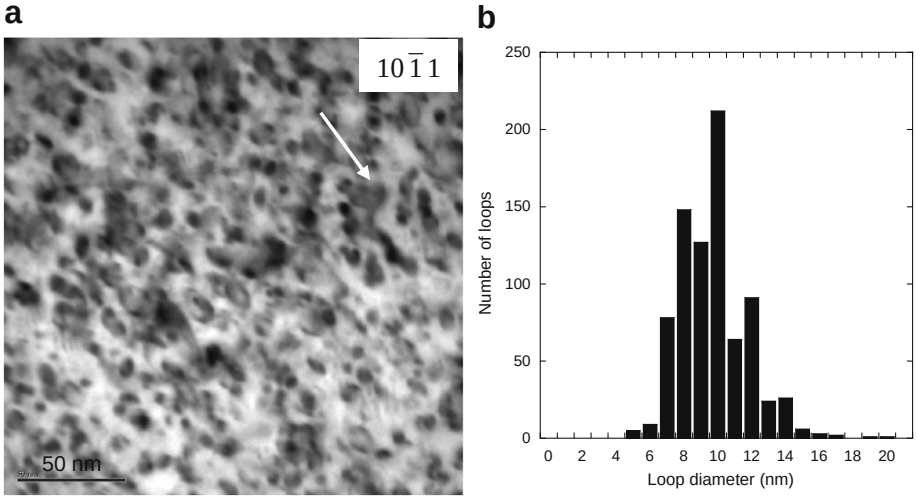

Fig. 4. (a) TEM micrograph of <a> dislocation loops at $g = 10\bar{1}1$ and (b) dislocation loop diameter distribution in Zircaloy-4 proton-irradiated to 2 dpa at 305 °C.

Table 3
Summary and literature comparison of radiation-induced microstructure and radiation-induced hardening characterization of Zircaloy-4 proton-irradiated to 2 dpa.

Material	Dose or fluence (dpa or n/m^2)	Temperature (°C)	Mean loop diameter (nm)	Mean loop density (m^{-3})	Hv unirradiated (kg mm^{-2})	Hv irr. (kg mm^{-2})	ΔHv (kg mm^{-2})
Zircaloy-4	2	305	10	17×10^{21}	206	250	44
Zircaloy-4 [15,16]	2	350	7	7×10^{21}	183	223	40
Zircaloy-4 [11]	0.6×10^{25}	280	10	10×10^{21}	–	–	–
Zircaloy-2 [21]	1×10^{25}	342	8.7	19×10^{21}	–	–	–

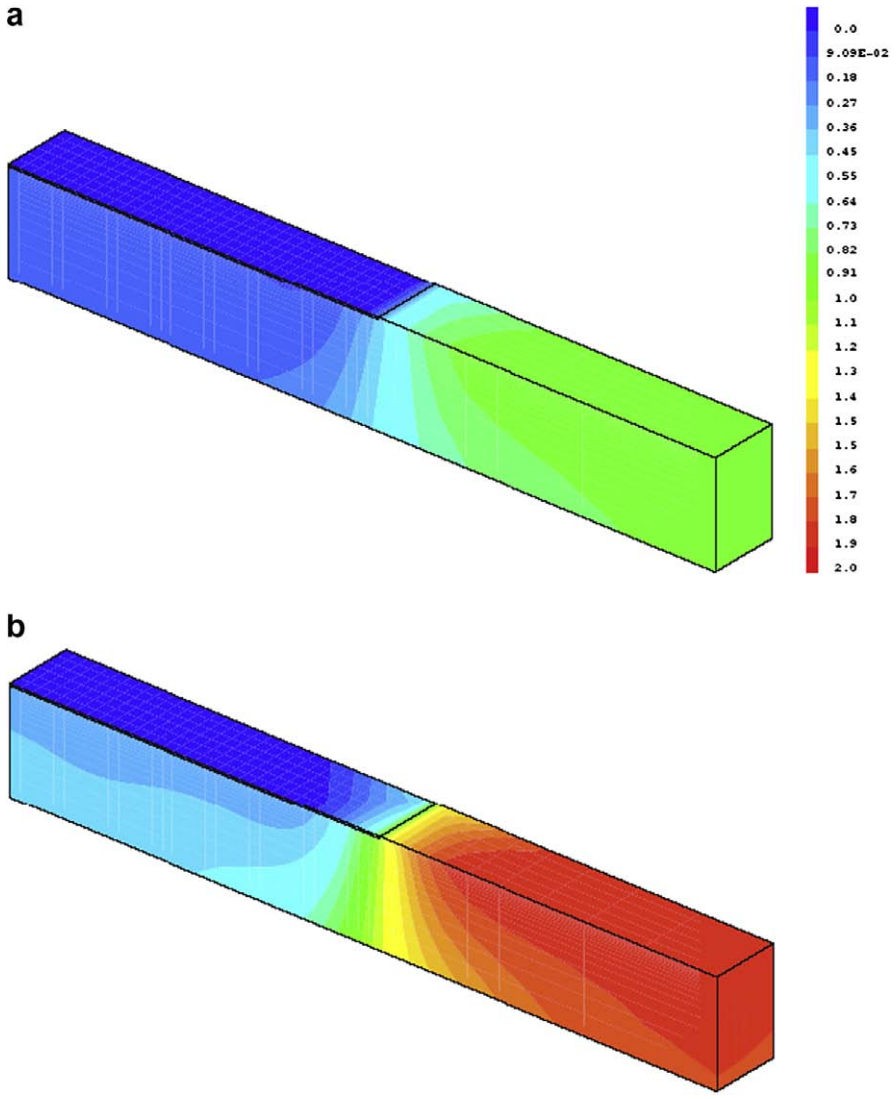

Fig. 5. Equivalent plastic strain (%) at (a) 0.5% macroscopic plastic strain and (b) 1.1% macroscopic plastic strain.

with the grain shown in Fig. 10(a) illustrate the identification of the slip orientation of the channels as basal. Basal channels mean width was determined to be 80 ± 10 nm.

4.4. Iodine-induced stress corrosion cracking

The results of the CERT tests performed at a strain rate of 10^{-5} s^{-1} and room temperature in iodized methanol solutions on unirradiated and irradiated Zircaloy-4 are summarized in Table 5. The strain-to-failure, failure mode, number of cracks and total crack length in both the unirradiated side surface and the irradiated side surface were tabulated for each specimen.

Initial CERT tests were performed in iodized methanol solutions at 10^{-6} g/g on both unirradiated (#1 and 2) and proton-irradiated (#3) specimens. All specimens failed in a fully transgranular ductile mode. The irradiated specimen exhibited numerous but shallow cracks on its irradiated side suggesting limited susceptibility to I-SCC. Surprisingly relative to specimens #1 and 2, the irradiated specimen also exhibited a few shallow cracks on its unirradiated side at 24% strain. Following tests were performed in methanol solutions with higher content in iodine, first at 4×10^{-6} g/g and then at 6×10^{-6} g/g.

The two unirradiated Zircaloy-4 specimens (#4 and 5) strained in iodized methanol solutions at 4×10^{-6} g/g did not exhibit environmentally assisted cracking. These specimens failed at a large strain, around 30%, in a transgranular ductile mode by microvoid coalescence. In contrast, the two proton-irradiated Zircaloy-4 specimens (#6 and 7) were found to be sensitive to SCC:

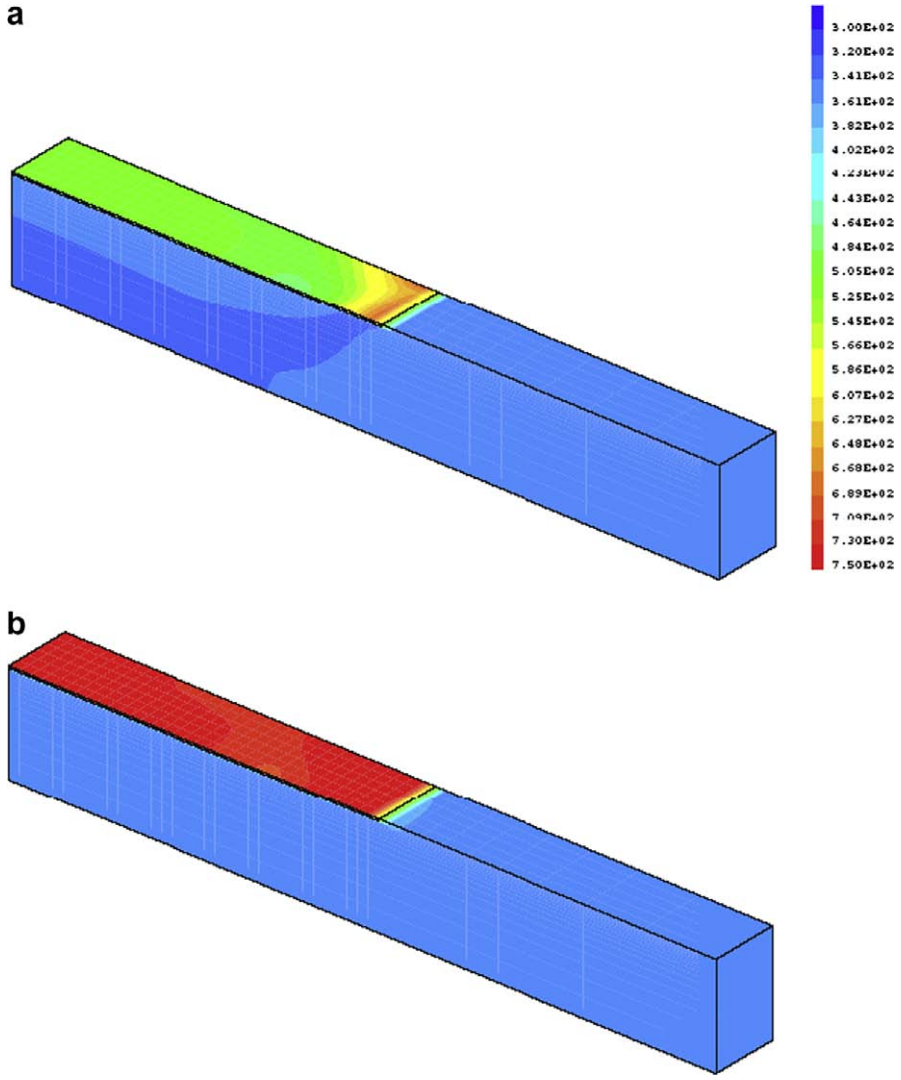

Fig. 6. Equivalent stress (MPa) at (a) 0.5% macroscopic plastic strain and (b) 1.1% macroscopic plastic strain.

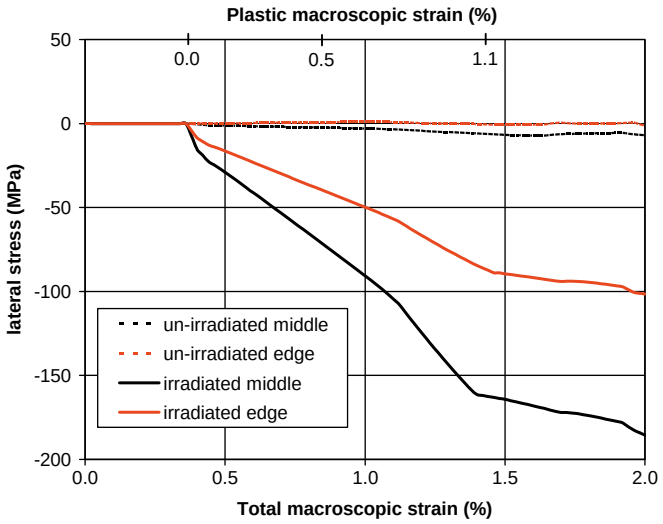

Fig. 7. Lateral stress in the center symmetry plan in the middle of the specimen and on the edge of the specimen, in the irradiated layer and in the un-irradiated part below the irradiated layer.

- In test #6, irradiation to 2 dpa was found to significantly promote SCC. As shown in Fig. 11(a) stress corrosion cracks have already initiated at the specimen's edges at 0.5% macroscopic plastic strain. Further straining of the specimen led to failure with an overall 20% loss of ductility in comparison to the unirradiated Zircaloy-4. SEM micrographs of the fracture surfaces for Zircaloy-4 proton-irradiated to 2 dpa are displayed in Fig. 11(b) and (c). Cracks are shown to have initiated in an intergranular mode at the specimen's edges (Fig. 11(b)) and to have propagated in a transgranular mode (Fig. 11(c)). A possible explanation for crack initiation at the specimen's edges is the significantly higher stress triaxiality ratio at the edge relative to the middle of the specimen shown by FE calculation in Section 4.2. A side-surface SEM micrograph of specimen # 6 strained to failure is displayed in Fig. 11(d). It should be noted the presence of macroscopic localized deformation bands 45° to the tensile axis in the irradiated region and the absence of these bands in the unirradiated region.
- Up to following the occurrence of crack initiation at specimen's edges in test #6, test #7 was conducted on a specimen proton-irradiated to 2 dpa with silicone paste protected edges and small side surfaces. This specific test was successively interrupted at 0.5%, 1%, 2% and 5% macroscopic plastic strain. No cracks were

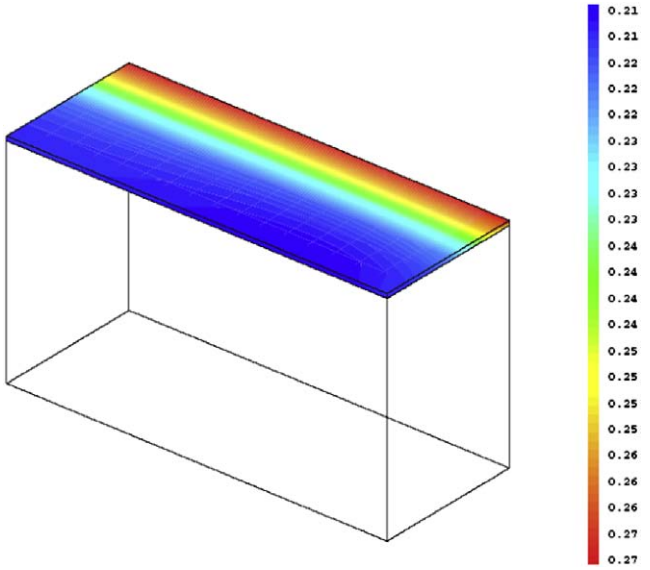

Fig. 8. Stress triaxiality ratio (ratio between hydrostatic stress and equivalent stress) in a portion of the irradiated layer at 1.1% macroscopic plastic strain. The depicted portion is at the center of the specimen, the under-laying un-irradiated specimen is depicted by its frame.

observed after 0.5% and 1% macroscopic plastic strain. In contrast, a few small cracks were observed on the unirradiated side of the specimen and several significant intergranular cracks with a 2000 μm total crack length were observed on the irradiated side of the specimen after 2% macroscopic plastic strain. SEM micrographs of the irradiated side surface of specimen #7 plastically strained to 2% are displayed in Fig. 12(a) and (b).

Like the unirradiated specimens strained in iodized methanol solutions at 10^{-6} g/g and 4×10^{-6} g/g, the unirradiated specimen #8 strained in iodized methanol solution at 6×10^{-6} g/g failed in a fully transgranular ductile mode. In contrast, the proton-irradiated specimen #9 with silicone paste protected edges and small side surfaces, exhibited stress corrosion cracks at macroscopic plastic strain as low as 0.5%.

All proton-irradiated specimens (#3, 6, 7, and 9) surprisingly exhibited stress corrosion cracks on their unirradiated side at various strain level depending on the iodine concentration of the methanol solution. Since all specimens were cleaned in methanol after irradiation, no obvious explanation was found during this work.

It should be highlighted here that the higher the iodine concentration of the methanol solution, the lower the strain to stress corrosion crack initiation. At 6×10^{-6} g/g, crack initiation occurs at 0.5% macroscopic plastic strain that approximately corresponds to an equivalent stress as low as 70% of the yield stress of the irradiated material in the proton-irradiated layer while no significant crack initiation is observed at 10^{-6} g/g.

5. Discussion

5.1. Channeling in proton-irradiated Zircaloy-4

Several authors already observed dislocation channeling in irradiated and deformed zirconium alloys [4–11]. Onimus et al. [10] recently proposed a TEM method to unambiguously determine channeling slip system in irradiated zirconium alloys and studied different loading conditions. These authors only observed basal channels after transverse tensile testing and closed end burst tests, and only prismatic and pyramidal channels after axial testing. In this study, channeling in Zircaloy-4 proton-irradiated to 2 dpa and strained in the transverse direction to 0.5% macroscopic plastic strain at a strain rate of 10^{-5} s^{-1} was investigated following the method proposed by Onimus et al. [10]. As presented in the results section, basal channels were mainly observed, in good agreement with the observations of Onimus et al. on neutron irradiated Zircaloy-4. Only one prismatic channel was observed in one grain with *c* axis close to the N direction. It should be emphasized here that channeling was characterized by Onimus et al. [10] after transverse tensile testing to approximately 0.4% plastic deformation while in

Table 4
Summary of strain localization characterization of Zircaloy-4 proton-irradiated to 2 dpa and strained to 0.5% macroscopic plastic strain at a strain rate of 10^{-5} s^{-1} at room temperature.

TEM foil studied	# of studied grains	# of grains with channels	Channeling plane	Mean number of channels per grain	Mean *B* channel width	Mean *P* channel width
1	12	4	*B*	5 ± 1	80 ± 10	–
2	28	7	*B* and *P*	2 ± 1	80 ± 10	40 ± 10

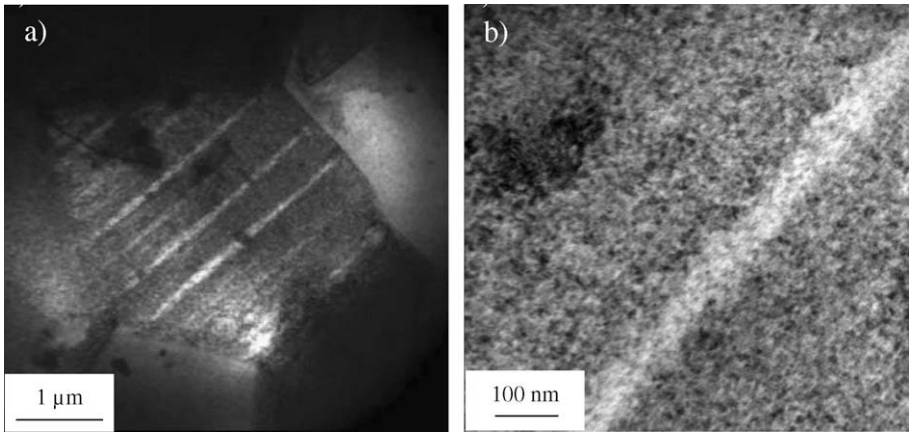

Fig. 9. (a)–(b) TEM micrographs of dislocation channels in Zircaloy-4 proton-irradiated to 2 dpa and strained to 0.5% macroscopic plastic strain at a strain rate of 10^{-5} s^{-1} at room temperature.

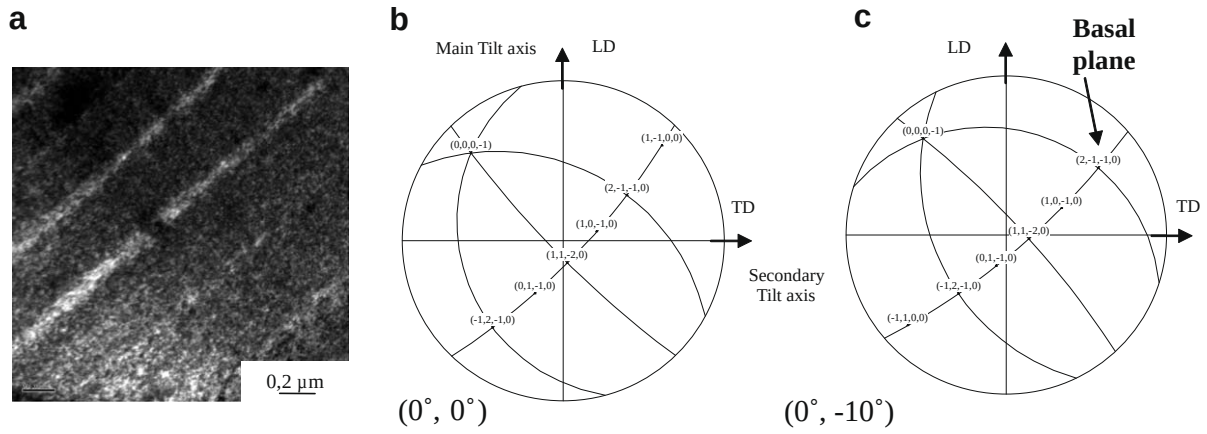

Fig. 10. (a) TEM micrograph showing basal channel in Zircaloy-4 proton-irradiated to 2 dpa and strained to 0.5% macroscopic plastic strain at a strain rate of 10^{-5} s^{-1} at room temperature. Stereographic projection of the grain imaged in (a) corresponding to (b) (0°,0°) tilt angles and (c) after (0°,−10°) tilt corresponding to the orientation of micrograph (a).

Table 5
Summary of CERT tests performed at a strain rate of 10^{-5} s^{-1} in iodized methanol solution at room temperature on unirradiated Zircaloy-4 as well as on Zircaloy-4 proton-irradiated to 2 dpa at 305 °C.

Specimen #	Dose (dpa)	Iodine conc. (g/g)	Macroscopic plastic strain to interruption (%)	Macroscopic strain to failure (%)	Failure mode	Side surface cracks			
						Unirradiated side		Irradiation side	
						Nb of cracks	Total crack length (fim)	Nb of cracks	Total crack length (fim)
1	Unirradiated	1×10^{-6}	–	26	TG ductile	0	0	–	–
2	Unirradiated	1×10^{-6}	–	27	TG ductile	0	0	–	–
3	2	1×10^{-6}	–	24	TG ductile	Notquantified		Notquantified	
4	Unirradiated	4×10^{-6}	–	30	TG ductile	0	0	–	–
5	Unirradiated	4×10^{-6}	–	28	TG ductile	0	0	–	–
6[a]	2	4×10^{-6}	0.5	–	–	0	0	10	670
			–	10	IG + TG	24	500	14	1380
7[b]	2	4×10^{-6}	0.5	–	–	0	0	0	0
			1	–	–	0	0	0	0
			2	–	–	4	60	99	2000
			5	–	–	8	120	163	3580
8	Unirradiated	6×10^{-6}	–	25	TG ductile	0	0	–	–
9[b]	2	6×10^{-6}	0.5	–	–	0	0	3	100
			1			2	30	10	310

[a] Crack inititation at specimen's edges.
[b] Specimen's edges and small side surfaces protected with silicone paste.

this study channeling was characterized in the micro-plasticity regime, at approximately 70% of the yield stress, suggesting that channeling can occur at stress levels well below the yield stress.

In order to further understand the transition from <a> dislocations glide in prismatic planes [22] to basal channeling with irradiation in the case of transverse tensile testing, maximum basal and prismatic Schmid factors were calculated for all the grains studied. The results of these calculations are displayed in Fig. 13. A clear distinction was made between (i) grains containing channels, (ii) grains without channel but with an orientation convenient for tilting so that the plane of interest (basel or prismatic) can contain the electron beam, and (iii) grains without visible channel, i.e. with an orientation unfavourable to tilt the plane of interest (basel or prismatic) so that it contains the electron beam. A strong correlation between high basal Schmid factor and the occurrence of basal channeling is seen in Fig. 13(a) with seven grains containing basal channels out of 22 well-oriented grains for basal slip. In contrast, prismatic channeling was found to occur in only one out of the 9 grains with maximum prismatic Schmid factor. These results are in good agreement with the observations of Onimus et al. [10] on neutron-irradiated Zircaloy-4 and also suggest that the basal critical resolved shear stress (CRSS) is lower than the prismatic CRSS after proton irradiation to 2 dpa, and that irradiation induces a change in the hierarchy of CRSS.

5.2. Influence of irradiation on I-SCC

This study was aimed at determining the influence of irradiation on I-SCC and giving insights into the possible effect of channeling on the phenomenon. The results presented in the previous section clearly demonstrate the detrimental effect of irradiation on I-SCC. In contrast, additional work is needed to investigate the mechanisms controlling the increased susceptibility of zirconium alloys to I-SCC after irradiation. In this work, no correlation could be made between the occurrence of basal channeling and I-SCC.

This study has also shown the presence of more macroscopic localized deformation bands 45° to the tensile axis in the irradiated region after CERT testing. The presence of these bands was also recently observed by Dexet [23] on unirradiated grade 702 zirconium alloy after transverse tensile testing at 4×10^{-4} s^{-1} and 200 °C to

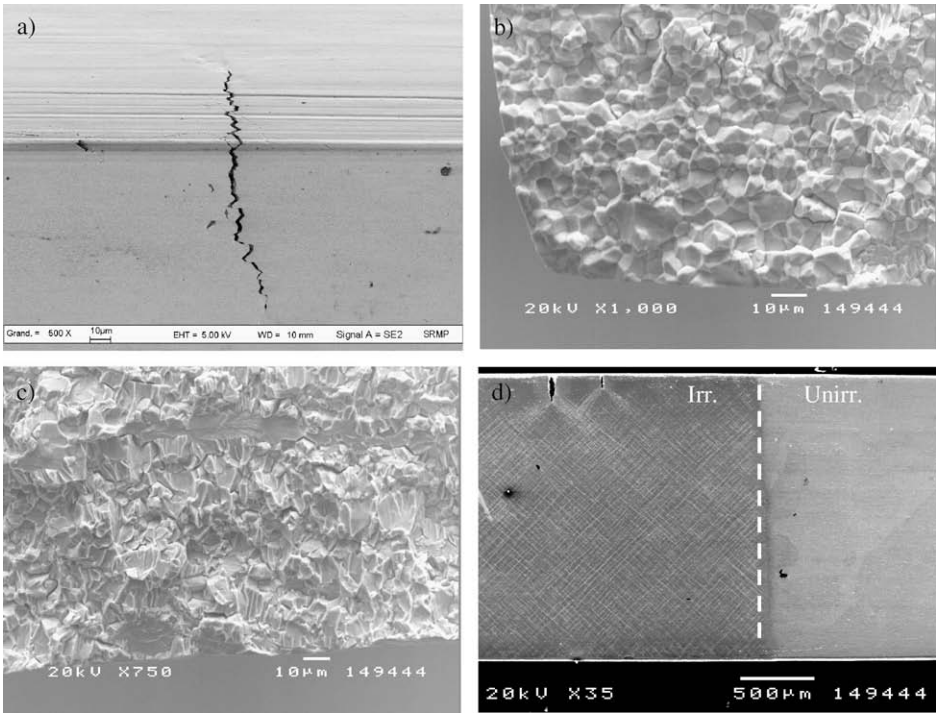

Fig. 11. SEM micrographs of (a) the side surface after straining to 0.5% plastic strain showing crack initiation at specimen's edge, (b)–(c) the fracture surface after straining to failure showing IG initiation and TG propagation, and (d) the side surface after straining to failure showing localized deformation bands 45° to the tensile axis in the irradiated region and the absence of these bands in the unirradiated region of proton-irradiated Zircaloy-4 specimen # 6.

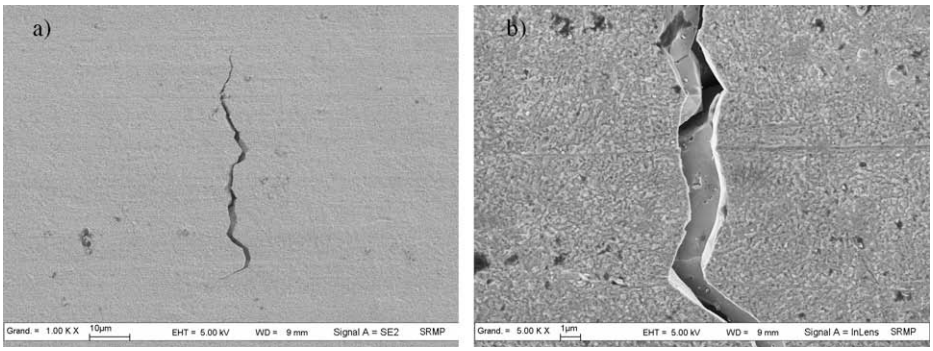

Fig. 12. (a)–(b) SEM micrographs of the side surface of proton-irradiated Zircaloy-4 specimen # 7 after straining to 2% plastic strain showing IG initiation.

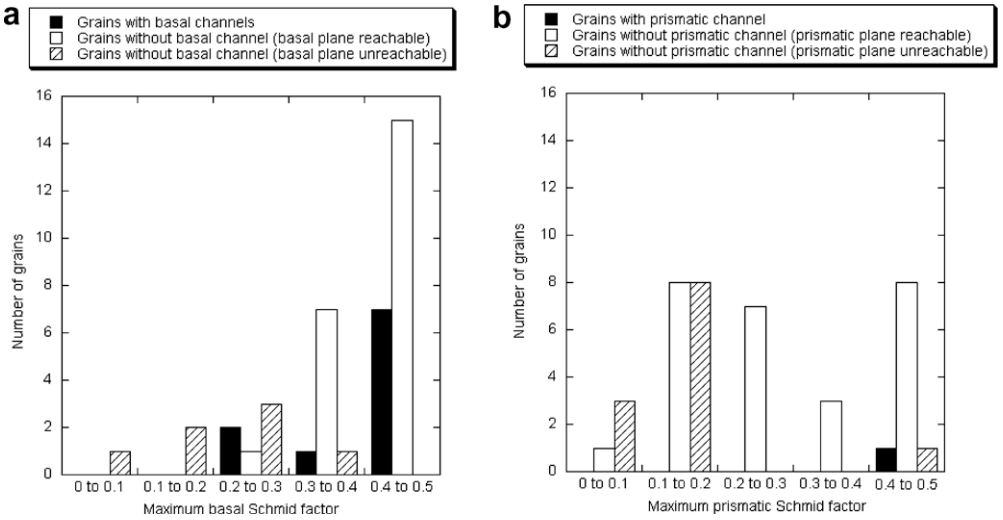

Fig. 13. Number of grains vs (a) maximum basal Schmid factor and (b) maximum prismatic Schmid factor for Zircaloy-4 proton-irradiated to 2 dpa and strained to 0.5% macroscopic plastic strain at a strain rate of 10^{-5} s^{-1} at RT.

2% plastic strain using micro-extensometry techniques. Further work is needed to determine if these bands contribute to I-SCC initiation by inducing high local stresses and strains at their intersections. In that regard, additional SCC tests using an alternative technique to CERT test may be particularly interesting since the formation of macroscopic localized deformation bands may be correlated with CERT testing.

6. Summary and conclusions

The radiation-induced microstructure, strain localization, and I-SCC behaviour of Zircaloy-4 proton-irradiated to 2 dpa at 305 °C was examined. The diameter and density of the <a> type dislocation loops and the increase of microhardness were similar to those observed after neutron irradiation. No $Zr(Fe,Cr)_2$ precipitates amorphization or Fe redistribution were observed after irradiation. Almost exclusively basal channeling was shown to occur for transverse tensile testing at a strain rate of $10^{-5}\,s^{-1}$ up to 0.5% macroscopic plastic strain at room temperature. Finite element calculations suggest that 0.5% macroscopic plastic strain corresponds to an equivalent stress close to 70% of the yield stress of the irradiated material in the proton-irradiated layer. Statistical Schmid factor analysis shows that irradiation induces a change in slip system activation from prismatic to basal via a change in the hierarchy of critical resolved shear stresses. Irradiation was found to strongly promote I-SCC. Strain to stress corrosion crack initiation was also found to decrease with an increase of the iodine concentration of the methanol solution.

Acknowledgments

Financial support was provided by CEA/DSOE-RB. The authors are grateful to CEZUS for providing the material, to O. Toader for his help in conducting proton irradiation at the University of Michigan Ion Beam Laboratory, and to researchers from CEA/SRMP for FEG-SEM examinations after SCC testing. Fruitful discussions with F. Onimus are also gratefully acknowledged.

References

[1] B. Cox, J. Nucl. Mater. 172 (1990) 249.
[2] I. Schuster, C. Lemaignan, J. Joseph, Nucl. Eng. Des. 156 (1995) 343.
[3] Y.K. Bibilashvili, A.V. Medvedev, B.I. Nesterov, V.V. Novikov, V.N. Golovanov, S.G. Eremin, A.D. Yurtchenko, J. Nucl. Mater. 280 (2000) 106.
[4] M. Fregonese, C. Régnard, L. Rouillon, T. Magnin, F. Levebvre, C. Lemaignan, in: Proceedings of the 12th International Symposium Zirconium in Nuclear Industry, ASTM STP 1354, 2000, p. 377.
[5] C.E. Coleman, D. Mills, J. van der Kuur, Can. Metall. Quater. 11 (1) (1972) 91.
[6] T. Onchi, H. Kayano, Y. Higashiguchi, J. Nucl. Mater. 88 (1980) 226.
[7] K. Petterson, J. Nucl. Mater. 105 (1982) 341.
[8] K. Farrell, T.S. Byun, N. Hashimoto, J. Nucl. Mater. 335 (2004) 471.
[9] R.B. Adamson, W.L. Bell, in: Proceedings of the International Symposium on Microstructure and Mechanical Behaviour of Materials, Xian, China, 1985, p. 237.
[10] F. Onimus, I. Monnet, J.L. Bechade, C. Prioul, P. Pilvin, J. Nucl. Mater. 328 (2004) 165.
[11] C. Régnard, B. Verhaegue, F. Lefebvre-Joud, C. Lemaignan, in: Proceedings of the 13th International Symposium Zirconium in Nuclear Industry, ASTM STP 1423, 2002, p. 384.
[12] T. Onchi, H. Kayano, Y. Higashiguchi, J. Nucl. Mater. 116 (1983) 211.
[13] J.C. Wood, J.R. Kelm, Res. Mechanica. 8 (1983) 127.
[14] G.S. Duffo, S.B. Farina, Corros. Sci. 47 (2005) 1459.
[15] X.T. Zu, M. Atzmon, L.M. Wang, L.P. You, F.R. Wan, G.S. Was, R.B. Adamson, J. ASTM Int. 1 (4) (2004) 741.
[16] X.T. Zu, K. Sun, M. Atzmon, L.M. Wang, L.P. You, F.R. Wan, J.T. Busby, G.S. Was, R.B. Adamson, Phil. Mag. 85 (4–7) (2005) 649.
[17] R. Limon, J.L. Bechade, S. Lehmann, R. Maury, A. Soniak, J.-P. Mardon, in: Proceedings of Le Zirconium – Journées d'Etudes "Propriétés-Microstructure", INSTN Saclay, Les Editions de Physique, 1995.
[18] S.T. Mahmood, K.L. Murty, J. Mater. Eng. 11 (4) (1989) 315.
[19] M. Nakatsuka, M. Nagai, J. Nucl. Sci. Technol. 24 (10) (1987) 832.
[20] P. Morize, J. Baicry, J.-P. Mardon, in: Proceeding of the 7th International Symposium Zirconium in the Nuclear Industry, ASTM STP 939, 1987, p. 101.
[21] D.O. Northwood, R.W. Gilbert, L.E. Bahen, P.M. Kelly, R.G. Blake, A. Jostsons, P.K. Madden, D. Faulkner, W. Bell, R.B. Adamson, J. Nucl. Mater. 79 (1979) 379.
[22] D.L. Douglass, in: Atomic Energy Review Supplement, International Atomic Energy Agency, 1971, p. 41.
[23] M. Dexet, PhD thesis, Ecole Polytechnique, France, 2006.